

2012 International Conference on Solid State Devices and Materials Science

Effect of Mn Doping on Structural and Optical Properties of SnO₂ Nanoparticles Prepared by Mechanochemical Processing

Nurul Syahidah Sabri, Mohd Salleh Mohd Deni, Azlan Zakaria, Mahesh Kumar Talari*

Faculty of Applied Sciences, Universiti Teknologi MARA, 40450 Shah Alam, Selangor, Malaysia

Abstract

SnO₂ is an n-type semiconductor with rutile crystalline structure and display many interesting optical properties. However, there are limited reports on effect of Mn doped SnO₂ on optical properties, prepared by mechanochemical processing. This paper reports the effect of Mn doping on structural and optical properties of SnO₂ nanoparticles (Sn_{1-x}Mn_xO₂, x = 0, 0.02, 0.04, 0.06, 0.08, 0.1) prepared by mechanochemical processing in a high energy ball mill and heat-treated at 600°C. Phase analysis of the dried powders was carried out from the data obtained by X-ray Diffraction (XRD) of the samples. The peak shifting in XRD patterns indicate that Mn ions were successfully doped into the SnO₂ crystal lattice with successive increase in dopant levels. Average crystallite size, was calculated based on Scherrer's equation, and was found to vary from 24 to 35 nm. Blue shift in E_g at x>0.02 may be affected by decrease in crystallite size. Red shift in E_g with increasing Mn concentration (x ≤ 0.02) could be attributed to either sp-d exchange interaction and to the increasing crystallite size of the SnO₂ nanoparticles. The quantum confinement effect was suggested to be the dominant reason for the changes in E_g. The reduction in emission intensity could be due to non-radiative recombination processes promoted by Mn ions with increasing Mn content.

© 2012 Published by Elsevier B.V. Selection and/or peer-review under responsibility of Garry Lee

Open access under [CC BY-NC-ND license](https://creativecommons.org/licenses/by-nc-nd/4.0/).

Keywords: Nanoparticles; SnO; Mn-doped SnO; Mechanochemical processing; Optical properties;

* Corresponding author. Tel.: +6-03-5521 1345; fax: "+6-03-5544 4562" .

E-mail address: talari@gmail.com.

1. Introduction

Many studies have been carried out in the area of the wide band gap semiconductor materials during last few years due to their potential use in short wavelength optical devices [1]. Tin oxide (SnO_2) is one of n-type wide-band-gap semiconductor material (3.6 eV) and has large exciton binding energy (130 meV) [2]. Furthermore, tin oxide also could be one of most promising candidates for Diluted Magnetic Semiconductor (DMS) materials, when 3d ions of magnetic transition metal impurities were replaced or substituted into cation sites of ZnO [3]. Mn ion could be a good candidate to replace Sn ion in SnO_2 lattice due to its larger thermal solubility (10 mol%) which can increase the amount of injected spins and carriers [4]. Which can make Mn doped SnO_2 as a promising material for spintronics application [5]. Most of studies paid attention on the magnetic properties of Mn doped SnO_2 (SMO) until now [6]. However, studies of effect Mn doped SnO_2 on optical properties are still lacking and need further research.

Nanosized doped SnO_2 have been prepared by several methods such as simple sol-gel method [7], chemical co-precipitation method [8], simple chemical precipitation method [9] and other methods. However, nanoparticles synthesized by the above methods are often expensive to produce nanoparticles in mass scales. Mechanochemical processing is an alternative economical method to produce the nanoparticles without serious agglomeration. In addition, studies on optical and structural properties of doped ZnO nanoparticles, prepared by mechanochemical processing are also still limited.

In this paper, structural and optical properties of $\text{Sn}_{1-x}\text{Mn}_x\text{O}_2$ nanoparticles prepared by mechanochemical processing are reported and the results are discussed in detail.

2. Method

Analytical grade SnCl_2 , Na_2CO_3 , NaCl and MnCl_2 were used as starting materials for the synthesis of SnO_2 and Mn doped SnO nanoparticles with a starting composition of $\text{Sn}_{1-x}\text{Mn}_x\text{O}$ ($x = 0, 0.02, 0.04, 0.06, 0.08, 0.1$). NaCl was used as diluents. The starting powder of the material were sealed in a 250 ml zirconium oxide vial along with 10 zirconium oxide balls of 20 mm diameter using a ball-to-powder weight ratio of 10:1 and was milled in a planetary mill for 5 hours at 500rpm. After 5 h of milling, the milled powders were heat-treated at 600°C for 1 h. NaCl was removed from the milled powders by selective leaching using deionised water as leachant and were dried at 100°C for 24 hours to obtain $\text{Sn}_{1-x}\text{Mn}_x\text{O}$ nanoparticles. X-Ray Diffraction (XRD) data was collected from Panalytical X-Ray diffractometer using $\text{Cu-K}\alpha$ radiation for phase identification and crystallite size calculation. The surface morphological analysis of the SnO and Mn doped SnO nanoparticles were investigated using Field Emission Scanning Electron Microscope (FESEM). Uv-Visible spectroscopic (Uv-Vis) technique was used for optical properties characterization of the samples. Energy gap (E_g) value of the samples was determined from Tauc plots using the relation

$$(\alpha h\nu)^2 = A (h\nu - E_g) \quad (1)$$

where α , A, $h\nu$ and E_g are absorption coefficient, constant, photon energy and energy gap (E_g). E_g was estimated from the intercept of the linear portion of the curve of $(\alpha h\nu)^2$ versus $h\nu$ plots [10].

3. Result and Discussion

3.1. Structural Properties

Figure 1 show the XRD patterns of $\text{Sn}_{1-x}\text{Mn}_x\text{O}_2$ nanoparticles which were heat-treated at 600°C . All the diffraction peaks were indexed and found to match with the JCPDS standard (No. 88-0287) data of rutile-type tetragonal structure of SnO_2 . The clear diffraction peaks shows that the nanoparticles are well crystalline. No trace of impurities phase such as manganese oxide or other tin oxides are detected in the XRD patterns. The diffraction peaks are observed to be shifting towards higher angles with increased Mn content which indicate that Mn ion has substituted the Sn site without changing the rutile structure. Lattice constant values were calculated from the XRD peak positions using least square method and shown in Figure 2. Lattice parameters and unit cell volume parameters are seen to decrease with the increased Mn content in the nanoparticles. The shrinkage of the lattice constant could be due to smaller ionic radius of Mn^{3+} (0.65 \AA) substituted in place of Sn^{4+} (0.69 \AA) site [8]. Figure 3 shows the crystallite size of $\text{Sn}_{1-x}\text{Mn}_x\text{O}_2$ nanoparticles, determined from the full width at half maximum (FWHM) of the XRD peaks using the Scherrer's formula [11] as function of the Mn content. The samples are nanoparticles with an average crystallite size lying in the range of 24-35 nm. Average crystallite size of nanoparticles was observed to increase at lower (at $x < 0.02$) Mn content and at higher Mn content ($x > 0.02$) crystallite size is seen to decrease. Decrease with the increasing Mn concentration may be caused by decreasing in diffusion rate with the increasing of dopant. Some quantity of Mn atoms may prefer to locate near or in crystal boundary regions when SnO_2 is doped with Mn and could hinder the growth of the crystals during the reaction in the ball mill resulting in decreased crystallite size [12]. Decreased in crystallite size with increasing Mn content also was observed by several researchers [9].

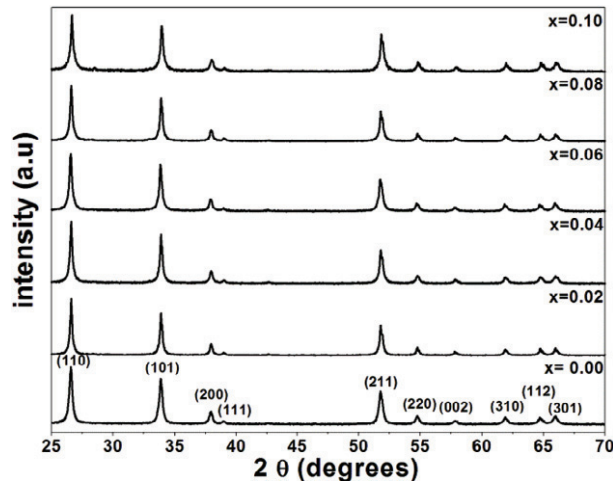


FIG. 1. XRD patterns of $\text{Sn}_{1-x}\text{Mn}_x\text{O}_2$ nanoparticles

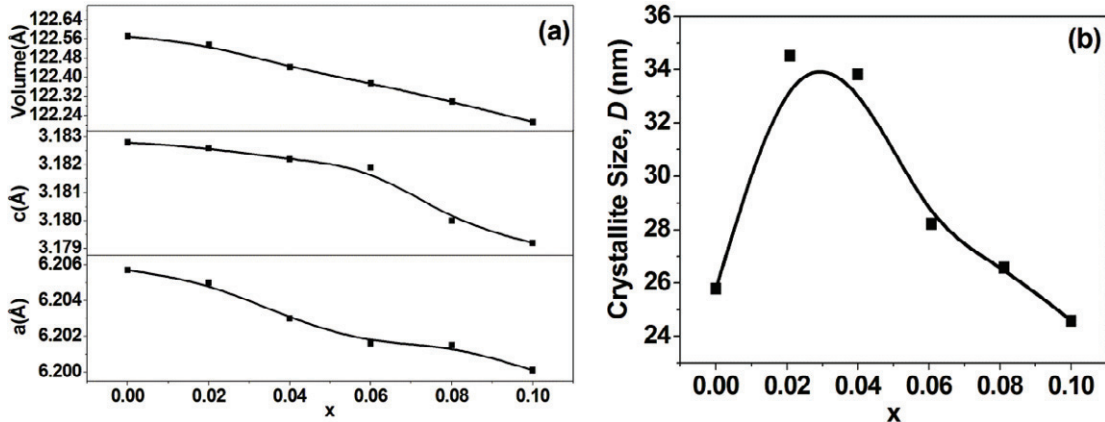


FIG. 2. (a) Lattice constant of $\text{Sn}_{1-x}\text{Mn}_x\text{O}_2$ nanoparticles; (b) Crystallite size of $\text{Sn}_{1-x}\text{Mn}_x\text{O}_2$ nanoparticles.

3.2. Optical Properties

Figure 4 presents the change in E_g as a function of Mn content and the inset shows the Tauc plots of $(\alpha h\nu)^2$ versus $h\nu$. The value E_g of SnO_2 nanoparticles (3.76 eV) is larger compared to value E_g of bulk SnO_2 (3.60 eV). The quantum confinement effect is expected increase the energy gap of semiconductor nanoparticles when the particle size decreases [7]. The E_g of Mn-doped SnO_2 is seen to decrease with the Mn doping, achieves a minimum value of 3.75 eV at $x=0.02$, and with further addition of Mn ($x>0.02$) energy gap displayed a blue shift. The blue shift in E_g could be attributed to the sp-d exchange interactions between the localized d electrons of Mn ions substituting Sn^{4+} and the band electrons [13]. On the other hand, the E_g of Mn-doped SnO_2 is found to be inversely proportional to the crystallite size nanoparticles due to the quantum confinement effect [14]. As can be seen from Figure 3, crystallite size increased up to $x \leq 0.02$ where as crystallite size decreased at $x = 0.04$ which correlates with sudden E_g increase at $x=0.04$ (Figure 4). It could be suggested that dominant reason of forthe shift in E_g is due to quantum confinement effect. Figure 5 shows the Fluorescence emission spectra of $\text{Sn}_{1-x}\text{Mn}_x\text{O}_2$ nanoparticles at 270nm excitation wavelength and the inset shows the emission spectrum of undoped SnO_2 nanoparticles fitted by Lorentzian peaks. Firstly, the emission peak of SnO_2 at 328nm (3.78 eV), could be assigned to the direct recombination of a conduction electron in the Sn '4p' and a hole in the O '2p' valence band since the value of emission is consistent with energy gap of SnO_2 nanoparticles. Secondly, the emission peak of SnO_2 , which was observed at 389nm (3.19 eV) probably correspond to the electron transition from the oxygen vacancies level to the valence band in SnO_2 nanoparticles [15]. Thirdly, the appearance of the strong emission peak at 419nm (2.96 eV) can be ascribed to the interactions between Sn vacancies and oxygen vacancies as suggested by Cheng et al. [16]. These interactions may result in the formation of trapped state as well as a series of metastable energy levels within the energy gap, thereby lead to strong emission at room temperature [16]. Fourth, the emission peak at 458nm (2.71 eV) might be due to electron transition mediated by defect levels such as oxygen vacancies in the energy gap [17]. In addition, the emission peak at 485nm (2.55 eV) is rarely found for SnO_2 and the emission near 485nm has been observed by Xu et al [15]. The emission should be from the defect generated during formation of SnO_2 nanoparticles. More theoretical work is needed to identify the origin of the observed emission. Based on the above discussion, the oxygen-related defects can be suggested to be most dominant defect centres in the emission of SnO_2 , which also have been supported by Gu et al. and Rani et al. [7, 18]. Emission intensity of $\text{Sn}_{1-x}\text{Mn}_x\text{O}_2$ nanoparticles are seen to reduce with the increasing Mn doping (Fig. 5). The reduction of emission intensity is related with the interaction among Mn ions and Mn ions may also tendency to cluster on the surface or on the grain boundaries of the

nanoparticles which could promote the non-radiative recombination processes [17]. Apart from non-radiative recombination, the reduction of emission intensity may due to the acceptor nature of Mn^{3+} ions with respect to Sn^{4+} ions in the SnO_2 nanoparticles. Doped Mn^{3+} ions may reduce donor type oxygen vacancies; hence reduce the intensity of oxygen vacancy related emission [18]. However, emission peak at 328nm doesn't involve any of the oxygen vacancy defects, also decreased significantly with increasing Mn. Thus, it can be suggested that non-radiative recombination is dominant phenomenon in the overall reduction in the emission intensity.

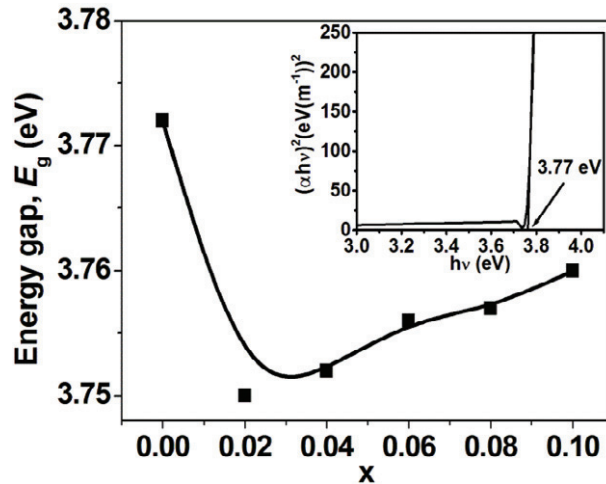


FIG. 3. The energy gap of $Sn_{1-x}Mn_xO_2$ nanoparticles. Inset shows plot of $(\alpha h\nu)^2$ versus $h\nu$.

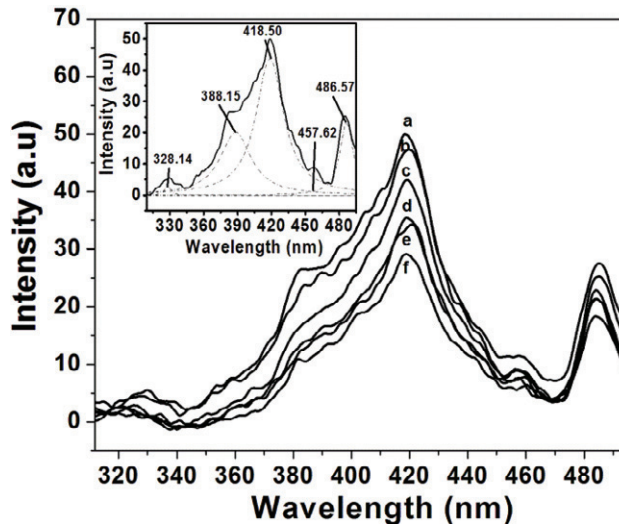


FIG. 4. Room temperature emission spectra for $Sn_{1-x}Mn_xO_2$ nanoparticles with an excitation wavelength of $\lambda_{exc} = 270$ nm: (a) SnO_2 , (b) $Sn_{0.98}Mn_{0.02}O_2$, (c) $Sn_{0.96}Mn_{0.04}O_2$, (d) $Sn_{0.94}Mn_{0.06}O_2$, (e) $Sn_{0.92}Mn_{0.08}O_2$ and (f) $Sn_{0.90}Mn_{0.10}O_2$. Inset shows the emission peaks of SnO_2 nanoparticles that were fitted by Lorentzian peaks.

4. Conclusion

Sn_{1-x}Mn_xO₂ nanoparticles have been successfully prepared by mechanochemical processing. The structural and optical properties of Sn_{1-x}Mn_xO₂ nanoparticles were studied using XRD and Uv-Vis. Mn substitution into the SnO₂ nanoparticles can be confirmed by the shifting of peaks in XRD patterns and shrinkage the lattice constant with increasing Mn content. The shift in E_g could be attributed to the sp-d exchange interactions or increase in crystallite size. Sudden decrease in crystallite size could have resulted in blue shift in E_g. In conclusion, it can be suggested that quantum confinement effect dominates the E_g behavior of Sn_{1-x}Mn_xO₂ nanoparticles. Except for the 328 nm emission, all other emissions are suggested to have originated from oxygen defects and mechanochemical processing is suggested to induce more defect centered emissions compared to the SnO₂ nanoparticles prepared by other synthesis methods. Mn doping resulted in the overall reduction of emission intensity which could be due to non-radiative recombination processes promoted by Mn ions.

References

- [1] Liu J, Zhang Y, Qi J., Huang Y, Zhang X, Liao Q. In-doped zinc oxide dodecagonal nanometer thick disks. *Mater. Lett.* 2006; **60**:2623-2626.
- [2] Liu B, Cheng CW, Chen R, Shen ZX, Fan HJ, Sun HD, Fine structure of ultraviolet photoluminescence of Tin Oxide nanowires. *J. Phys. Chem. C* 2010; **114**: 3407–3410.
- [3] Viswanatha R, Sapra S, Gupta SS, Satpati B, Satyam PV, Dev BN, Sarma DD. Synthesis and characterization of Mn-doped ZnO nanocrystals. *J. Phys. Chem. B* 2004; **108**:6303-6310.
- [4] Sharma P, Gupta A, Owens FJ, Inoue A, Rao KV. Room temperature spintronic material—Mn-doped ZnO revisited. *J. Magn. Magn. Mater.* 2004; **282**:115-121.
- [5] Wang YS, Thomas PJ, O'Brien P. Optical Properties of ZnO nanocrystals doped with Cd, Mg, Mn, and Fe ions. *J. Phys. Chem. B* 2006; **110**:21412-21415.
- [6] .G. Chen, W.W. Li, J.D. Wu, J. Sun, K. Jiang, Z.G. Hu, J.H. Chu. Temperature dependence of electronic band transition in Mn-doped SnO₂ nanocrystalline films determined by ultraviolet-near-infrared transmittance spectra. *Mater. Research Bulletin* 2012; **47**:111–116
- [7] Gu F, Wang SF, Song CF, Lu MK, Qi YX, Zhou GJ, Xu D, Yuan DR, Synthesis and luminescence properties of SnO₂ nanoparticles. *Chem. Phys. Lett.* 2003; **372**; 451–454.
- [8] Tian ZM, Yuan SL, He JH, Li P, Zhang SQ, Wang CH, Wang YQ, Yin SY, Liu L. Structure and magnetic properties in Mn doped SnO₂ nanoparticles synthesized by chemical co-precipitation method. *J. Alloys Compd.* 2008; **466**:26–30.
- [9] Sathyaseelan B, Senthilnathan K, Alagesan T, Jayavel R, Sivakumar K. A study on structural and optical properties of Mn- and Co-doped SnO₂ nanocrystallites. *Mater. Chem. Phys.* 2010; **124**:1046–1050.
- [10] Sethikumar S, Rajendran K, Banerjee S, Chini TK, Sengodan V. Influence of Mn doping on the microstructure and optical property of ZnO. *Mat. Sci. Semicon. Proc.* 2008; **11**:6-12.
- [11] Papadopoulou EL, Varda M, Kouroupis-Agalou K, Androulidaki M, Chikoidze E, Galtier P, Huyberechts G, Aperathitis E. Undoped and Al-doped ZnO films with tuned properties grown by pulsed laser deposition. *Thin Solid Films* 2008; **516**:8141–8145.
- [12] Sabri NS, Yahya AK, Talari MK, Structural and Optical Properties: Mn Doped Nano ZnO Synthesized by Mechanochemical Synthesis. *AIP Con. Proc.* 2010; **1250**:436-439.
- [13] X.G. Chen, W.W. Li, J.D. Wu, J. Sun, K. Jiang, Z.G. Hu, J.H. Chu. Temperature dependence of electronic band transition in Mn-doped SnO₂ nanocrystalline films determined by ultraviolet-near-infrared transmittance spectra. *Mater. Research Bulletin* 2012; **47**:111–116
- [14] Valle GG, Hammer P, Pulcinelli SH, Santilli CV. Transparent and conductive ZnO:Al thin films prepared by sol-gel dip coating. *J. Eur. Ceram. Soc.* 2004; **24**:1009–1013.

- [15] Xu J, Yang H, Fu W, Fan W, Zhu Q, Li M, Zou G, Synthesis and characterization of stainless steel/tin oxide: Bifunctional magnetic-optical nanocomposites. *Mater. Sci. Eng. B* 2007;**140**:132–136.
- [16] Cheng C, Xu G, Zhang H, Li Y, Luo Y, Zhang P, A simple route to synthesize multiform structures of tin oxide nanobelts and optical properties investigation. *Mater. Sci. Eng. B* 2008;**147**:79–83.
- [17] Gu F, Wang SF, Lu MK, Zhou GJ, Xu D, Yuan DR, Photoluminescence Properties of SnO₂ Nanoparticles Synthesized by Sol-Gel Method. *J. Phys. Chem. B* 2004;**108**: 8119-8123.
- [18] Rani S, Roy SC, Karar N, Bhatnagar MC, Structure, microstructure and photoluminescence properties of Fe doped SnO₂ thin films. *Solid State Communications* 2007;**141**: 214-218.